

Case Report

Susceptibility weighted imaging in a case of lissencephaly: Evidence of persistent fetal vasculature

Vinay S. Hegde^a, Jitender Saini^{a,*}, Ananta Ram^a, Paramveer S. Sabharwal^a and Parayil S. Bindu^b

^a*Department of Neuroimaging and Interventional Radiology, National Institute of Mental Health and Neurosciences (NIMHANS), Bangalore, India*

^b*Department of Neurology, National Institute of Mental Health and Neurosciences (NIMHANS), Bangalore, India*

Received 24 March 2013

Revised 28 May 2013

Accepted 9 June 2013

Abstract. Lissencephaly, with posterior-anterior gradient, are congenital brain malformations characterized by the presence of a few broad, flat gyri with thickened cortex. It results from the arrest of neuronal migration in early gestation. Magnetic resonance imaging (MRI) findings are characteristic and show thickened dysplastic cortex with a paucity of gyri and sulci. We report a case of lissencephaly with posterior-anterior gradient with unique imaging findings on susceptibility weighted imaging. Susceptibility weighted imaging revealed prominent venous channels traversing the thickened cortex. These channels possibly represent primitive vessels, similar to those seen in early cortical development, and can probably be seen due to the enormously thickened cortex in case of lissencephaly.

Keywords: Lissencephaly, susceptibility weighted imaging, persistent fetal vasculature

1. Introduction

Lissencephaly with posterior-anterior gradient is an uncommon malformation of cortical development classified as a malformation due to abnormal neural migration. Other disorders of similar underlying pathogenesis include cobblestone complex and heterotopias and few types of focal cortical dysplasias [1,2]. Histologically, classic lissencephaly shows four cortical layers instead of normal six layers [2]. Malformations of cortical development are also known to be associated

with both macrovascular [3–5] and microvascular [6] abnormalities of neuroparenchyma.

Imaging plays an important role in the diagnosis of this rare condition [7]. Conventional (MRI) sequences, e.g., T1-weighted, T2-weighted and fluid-attenuated inversion recovery are used for routine clinical imaging of brain malformations. Susceptibility weighted imaging (SWI), utilizes phase-encoded information to create a new unique tissue contrast. SWI is exquisitely sensitive to iron, both in cortical layers and in blood vessels, thereby revealing structures that were not identifiable previously on MRI [8,9]. In SWI, deoxygenated blood-rich small veins, which are smaller than the actual voxel size, can be identified due to an out-of-phase partial volume signal cancellation mechanism [10]. This unique ability of SWI to detect small vascular structures with great sensitivity has allowed detection of additional

*Corresponding author: Dr. Jitender Saini, DM, Department of Neuroimaging and Interventional Radiology, National Institute of Mental Health and Neurosciences (NIMHANS), Hosur Road, Bangalore 560029, India. Tel.: +91 80 26560024; +91 948 082 9654; Fax: +91 80 26564830; E-mail: jsaini76@gmail.com.

abnormalities in various clinical conditions resulting in increased sensitivity as well as better understanding of the underlying pathophysiology. Clinically, SWI is increasingly being utilized in the evaluation of many disease processes [11], including trauma, neurovascular disease, neurodegenerative disorders, multiple sclerosis, and neoplasms. Recently SWI has been found useful in cases of cortical malformation [12]. In this report, we describing a new observation on SWI in a case of lissencephaly. To the best of our knowledge, this is a novel finding and has not been reported previously.

2. Case report

A 4-year-old boy, the second child of non-consanguineous parents, presented with developmental delay and uncontrolled seizures beginning at 9 months of age. He had a normal birth and perinatal history with a birth weight of 3.5 kg. The seizures were characterized by sudden head drops and myoclonic jerks, which occurred with a frequency of 2–3 episodes per day. The seizures remained uncontrolled on optimal dosages of sodium valproate and clonazepam at the time of presentation. He had gross cognitive impairment. On examination, the child was alert with good visual tracking and response to sound. He had no dysmorphic features or neurocutaneous markers. He had microcephaly (head circumference 47 cm, less than 3rd percentile), nystagmus, hypotonia of all four limbs and showed brisk stretch reflexes with bilateral extensor plantars. Ophthalmological examination revealed a normal fundus. The routine laboratory work-up revealed normal blood counts, erythrocyte sedimentation rate, normal urea, creatinine, glucose, calcium, phosphate, alkaline phosphatase, liver function tests, serum lactate and ammonia levels. His urine was negative for any abnormal metabolites, and tandem mass spectrometry revealed normal amino acids and acyl-carnitine profile. Electroencephalography showed highly recurrent epileptiform discharges in the form of runs of sharp waves and spike-wave complexes predominantly from bilateral posterior leads with a normal intervening background.

Image acquisition: MRI was performed on an Aera 1.5T MRI scanner (Siemens Medical Systems, Erlangen, Germany) with a 20-channel head coil. MRI was done under sedation after prior parental informed consent. The MRI scans were obtained by first performing a three plane localizer scan, followed by an axial turbo spin-echo T2-weighted scan (repetition time [TR]/echo time [TE] 3270/80 ms, flip angle 90°, field of view [FOV] 250 × 250 mm, acquisition

[ACQ] voxel size 0.89/1.21/5.00 mm, slice thickness/gap 5/1 mm); T2 weighted fluid-attenuated inversion recovery (TR/TE 11000/120 msec, flip angle 90°, FOV 250 × 250 mm, ACQ voxel size 0.96/1.79/5.00 mm, slice thickness/gap 5/1 mm). Three dimensional magnetization-prepared rapid acquisition gradient-echo volumetric acquisition of the whole brain was acquired (TR/TE = 8.3/3.8 ms, sense factor = 1.5, flip angle = 8°, FOV = 256, ACQ voxel size 1/1/1 mm). SWI was acquired using TR = 49 ms, TE = 40 ms, flip angle = 15°, bandwidth = 80 kHz, matrix size = 512 × 256, slice thickness = 2 mm with 56 slices in a single slab, and integrated parallel acquisition techniques factor = 2. The acquisition time was 2 min 27 sec. Postprocessing was performed, and 12 mm thick minimum intensity projection slabs of 2 mm thickness were generated.

3. Results

Routine MRI revealed markedly reduced gyrii with a relatively smooth brain surface involving the posterior part of the brain including the occipital lobe, posterior temporal and parietal lobes (Fig. 1). The cortex was markedly thickened in most of the cerebral

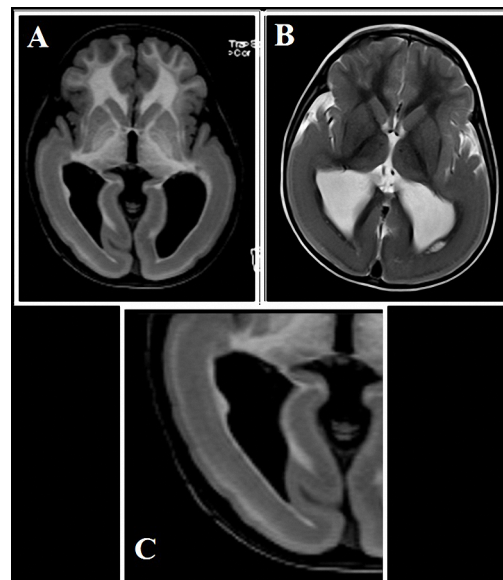


Fig. 1. Axial T1 magnetization-prepared rapid acquisition gradient-echo T2-weighted images (A) and T2-weighted images T1 magnetization-prepared rapid acquisition gradient-echo (B) images showing pachygryia involving occipital lobe, posterior temporal and parietal lobes of both cerebral hemispheres. A zoomed-out image of T1 magnetization-prepared rapid acquisition gradient-echo (C) shows three distinct layers with different signal intensities appreciated in the thickened cerebral cortex on careful inspection.

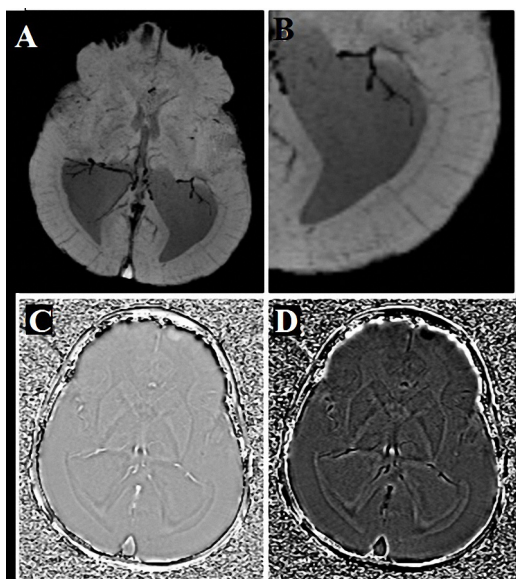


Fig. 2. Susceptibility weighted imaging minimum intensity projection images (A, B), filtered phase image (B,C), inverted phase image (D) magnitude image (C) and magnified minimum intensity projection image (D) revealing abnormal vascular channels running radially across the thickened cortex reaching up to the brain surface. These radially oriented vessels are seen as hypointense on minimum intensity projection (A,B) and inverted phase image (D) and hyperintense on phase image (C).

hemispheres with relative sparing of the frontal areas. Gray-white matter distinction was poor in places. On careful inspection of T1-weighted and T2-weighted images, three distinct layers with different signal intensities could be appreciated in the thickened cerebral cortex (Fig. 1C). A thin layer could be seen on both T1-weighted and T2-weighted images splitting the cortex into thin superficial and thick deeper layers. Cerebellum, vermis and brainstem appeared normal. SWI images revealed abnormal vascular channels running across the thickened cortex reaching up to the brain surface: numerous channels were seen throughout the thickened cortex (Figs. 2A–D).

4. Discussion

SWI has been reported to be useful in patients with cortical malformations [12]. It can show abnormal gray-white matter junction and may also detect associated vascular abnormalities with increased sensitivity. The present report highlights the utility of SWI in demonstrating the radially oriented venous channels in a patient with lissencephaly with posterior-anterior gradient.

In the early mammalian embryo the blood vessels of the developing cerebral cortex are in the form of loops or arcades with large perforating arteries and veins penetrating the cortex and subjacent white matter [13]. They give branches which join the deeper aspect of the perforating vessels. During development there is a progressive elaboration of this vascular arcade and it evolves into a reticular type of vascular system. New capillaries emerge from the perforating vessels and form an anastomosis between them. This changes the arrangement from a predominantly radial one to a complex reticular pattern. This complex capillary network leads to increased vascularity of the developing brain and it is dynamic in nature with capillaries undergoing continuous change in the form of active angiogenesis and reabsorption [14–16]. Developmental changes in the microvasculature of the cortex are further determined by the functional needs of the neurons. Possibly various growth factors and other biomolecules interact in a complex fashion to couple the development of the normal cortex with its microvasculature [15]. When there is maldevelopment of the cortex due to various factors it might result in abnormal development of the cortical microvasculature [15]. In our subject we could observe radially-oriented vascular channels in the abnormally thickened cortex and, since they appeared hypointense on minimum intensity projection images and hyperintense on phase images, we considered them likely to be veins. Given the sensitivity of SWI to vascular structures, an abnormal vascular pattern would be the most likely explanation for the radially-oriented linear structures observed in our patient.

Noninvasive confirmation of the venous structures could be done with a modulation of blood oxygenation by breathing a mixture of air, carbogen, and oxygen and then directly visualize the effects of changing blood oxygenation on the magnetic field inside and around the venous blood vessels on high-resolution SWI [18]. However, such a study could not be performed in our subject. This novel observation needs further exploration by histopathological studies which may confirm the nature of the microvascular abnormalities in patients with abnormal cortical development.

References

- [1] Barkovich AJ, Kuzniecky RI, Jackson GD, Guerrini R, Dobyns WB. A developmental and genetic classification for malformations of cortical development. *Neurology* 2005; 65(12):1873–87.

- [2] Barkovich AJ. Congenital malformations of the brain and skull. In: Barkovich AJ, editor. Paediatric neuroimaging 4th ed, vol 1. Philadelphia: Lippincott Williams&Wilkins; 2005. p. 346.
- [3] Rasalkar DD, Paunipagar BK. Developmental venous anomaly associated with cortical dysplasia. *Pediatr Radiol* 2010; 40(Suppl 1):S165.
- [4] Barkovich AJ. Abnormal vascular drainage in anomalies of neuronal migration. *AJNR Am J Neuroradiol* 1988;9(5):939–42.
- [5] Watanabe M, Tanaka R, Takeda N, Ikuta F, Oyanagi K. Focal pachygryria with unusual vascular anomaly. *Neuroradiology* 1990;32(3):237–40.
- [6] Kakita A, Hayashi S, Moro F, Guerrini R, Ozawa T, Ono K, et al. Bilateral periventricular nodular heterotopia due to filamin 1 gene mutation: widespread glomeruloid microvascular anomaly and dysplastic cytoarchitecture in the cerebral cortex. *Acta Neuropathol* 2002;104(6):649–57.
- [7] Abdel Razek AA, Kandell AY, Elsorogy LG, Elmongy A, Basett AA. Disorders of cortical formation: MR imaging features. *AJNR Am J Neuroradiol* 2009;30(1):4–11.
- [8] Haacke EM, Mittal S, Wu Z, Neelavalli J, Cheng YC. Susceptibility-weighted imaging: technical aspects and clinical applications, part 1. *AJNR Am J Neuroradiol* 2009;30(1):19–30.
- [9] Reichenbach JR, Venkatesan R, Schillinger DJ, Kido DK, Haacke EM. Small vessels in the human brain: MR venography with deoxyhemoglobin as an intrinsic contrast agent. *Radiology* 1997;204(1):272–7.
- [10] Sehgal V, Delproposto Z, Haacke EM, Tong KA, Wycliffe N, Kido DK, et al. Clinical applications of neuroimaging with susceptibility-weighted imaging. *J Magn Reson Imaging* 2005;22(4):439–50.
- [11] Thomas B, Somasundaram S, Thamburaj K, Kesavadas C, Gupta AK, Bodhey NK, et al. Clinical applications of susceptibility weighted MR imaging of the brain - a pictorial review. *Neuroradiology* 2008;50(2):105–16.
- [12] Madan N, Grant PE. New directions in clinical imaging of cortical dysplasias. *Epilepsia* 2009;50 Suppl 9:9–18.
- [13] Raybaud C. Normal and abnormal embryology and development of the intracranial vascular system. *Neurosurg Clin N Am* 2010;21(3):399–426.
- [14] Lewis OJ. The form and development of the blood vessels of the mammalian cerebral cortex. *J Anat* 1957;91(1):40–6.
- [15] Marín-Padilla M. The human brain intracerebral microvascular system: development and structure. *Front Neuroanat* 2012;6(9):38.
- [16] Allsopp G, Gamble HJ. Light and electron microscopic observations on the development of the blood vascular system of the human brain. *J Anat* 1979;128(Pt 3):461–77.
- [17] Raybaud C, Widjaja E. Development and dysgenesis of the cerebral cortex: malformations of cortical development. *Neuroimaging Clin N Am* 2011;21(3):483–543.
- [18] Rauscher A, Sedlacik J, Barth M, Haacke EM, Reichenbach JR. Noninvasive assessment of vascular architecture and function during modulated blood oxygenation using susceptibility weighted magnetic resonance imaging. *Magn Reson Med* 2005;54(1):87–95.